ACS APPLIED MATERIALS & INTERFACES

Biological and Medical Applications of Materials and Interfaces

Antimicrobial photodynamic polymeric films bearing biscarbazol-triphenylamine end-capped dendrimeric Zn(II) porphyrin

Daniel Heredia, Sol R. Martínez, Andrés M. Durantini, María Eugenia Pérez, María Inés Mangione, Javier E. Durantini, Miguel Gervaldo, Luis Alberto Otero, and Edgardo Néstor Durantini

ACS Appl. Mater. Interfaces, **Just Accepted Manuscript** • DOI: 10.1021/acsami.9b09119 • Publication Date (Web): 16 Jul 2019

is published by the American Chemical Society. 1155 Sixteenth Street N.W., Washington, DC 20036

Antimicrobial Photodynamic Polymeric Films Bearing Biscarbazol-Triphenylamine End-Capped Dendrimeric Zn(II) Porphyrin

Daniel A. Heredia,[1⊥] Sol R. Martínez,[1⊥] Andrés M. Durantini,[1⊥] M. Eugenia Pérez,[1⊥] María I. Mangione,[2⊥] Javier E. Durantini,[3⊥] Miguel A. Gervaldo,[3] Luis A. Otero,[3] Edgardo N. Durantini[1*]

[1] IDAS-CONICET, Departamento de Química, Facultad de Ciencias Exactas, Físico-Químicas y Naturales, Universidad Nacional de Río Cuarto, Ruta Nacional 36 Km 601, X5804BYA Río Cuarto, Córdoba, Argentina.

[2] IQUIR-CONICET, Facultad de Ciencias Bioquímicas y Farmacéuticas, Universidad Nacional de Rosario, Suipacha 531, S2002LRK Rosario, Argentina.

[3] IITEMA-CONICET, Departamento de Química, Facultad de Ciencias Exactas, Físico-Químicas y Naturales, Universidad Nacional de Río Cuarto, Ruta Nacional 36 Km 601, X5804BYA Río Cuarto, Córdoba, Argentina.

* Corresponding author. Tel.: +54 358 4676157; fax: +54 358 4676233.

E-mail address: edurantini@exa.unrc.edu.ar (E.N. Durantini)

Abstract

A novel biscarbazol-triphenylamine end-capped dendrimeric zinc(II) porphyrin (**DP 5**) was synthesized by click chemistry. This compound is a cruciform dendrimer, which bears a nucleus of zinc(II) tetrapyrrolic macrocycle substituted at the *meso* positions by four identical substituents. These are formed by a tetrafluorophenyl group that possess in the *para* position a triazole unit. This nitrogenous heterocyclic is connected to a 4,4'-di(*N*-carbazolyl)triphenylamine group by means of a phenylenevinylene bridge, which allows the conjugation between the nucleus and this external electropolimerizable carbazoyl group. In this structure, dendrimeric arms act as light-harvesting antennas, increasing the absorption of blue light and as electroactive moieties. The electrochemical oxidation of the carbazole groups contained in the terminal arms of the **DP 5** was used to obtain novel stable and reproducible fully π-conjugate photoactive polymeric films (**FDP 5**). First, the spectroscopic characteristics and photodynamic properties of **DP 5** were compared with its constitutional components derived of porphyrin **P 6** and carbazole **D 7** moieties in solution. The fluorescence emission of the dendrimeric units in **DP 5** were strongly quenched by the tetrapyrrolic macrocycle, indicating photoinduced energy transfer. In addition, **FDP 5** film showed the Soret and Q absorption bands and red fluorescence emission of the corresponding zinc(II) porphyrin. Also, **FDP 5** film was highly stable to photobleaching and it was able to produce singlet molecular oxygen in both *N*,*N*-dimethylformamide and water. Therefore, the porphyrin units embedded in the polymeric matrix of **FDP 5** film mainly retain the photochemical properties. Photodynamic inactivation mediated by **FDP 5** film was investigated in *Staphylococcus aureus* and *Escherichia coli*. When a cell suspension was deposited on the surface, complete eradication of *S. aureus* and a 99% reduction in *E. coli* survival were found after 15 min and 30 min irradiation, respectively. Also, **FDP 5** film was highly effective to eliminate individual bacteria attached to the surface. In addition, PDI sensitized by **FDP 5** film produced more than 99.99% bacterial killing in biofilms formed on the surface after 60 min irradiation. The results indicate that **FDP 5** film

represents an interesting and versatile photodynamic active material to eradicate bacteria as planktonic cells, individual attached microbes or biofilms.

Keywords: polymeric films; click chemistry; porphyrin; carbazole; photodynamic inactivation; antibacterial surface.

Introduction

Nosocomial infections are one of the main causes of avoidable harm in hospital patients and a substantial and unnecessary loss of health resources.[1] Treatments for these diseases can cause prolonged hospitalization, additional studies and antimicrobial medication, which leads to a considerable increase in the costs of medical care.[2] Although, diseases can be caused by a wide variety of microorganisms, a few of them are mainly responsible for infections acquired in the hospital.[3] In particular, *Staphylococcus aureus* is considered one of the most important pathogens responsible for nosocomial infections.[4] In addition, *Escherichia coli* is an emerging nosocomial pathogen producing problems in health care settings. Therefore, the control of the microorganisms responsible for hospital-acquired infections is very necessary since they cause an important economic and production loss. Therefore, it is essential to propose new methodologies for prophylaxis in areas of high risk for the contagion of nosocomial infections.[5] For this purpose, photodynamic inactivation (PDI) of microorganisms has been planned as an alternative methodology to eliminate bacterial diseases. This therapy uses a photosensitizer, visible light and oxygen to produce highly reactive oxygen species (ROS), which can react with several cell components. These molecular modifications induce a loss of biological functionality that cause cell death. In this method, two mechanisms can take place after activation of the photosensitizer.[6] Thus, the interaction of the excited photosensitizer with different substrates can form radicals, which can react with oxygen producing ROS, known as type I photoprocess. On the other hand, in a type II pathway the photosensitizer can transfer energy from its triplet excited state to produce singlet molecular oxygen, $O_2(^1\Delta_g)$.

In most PDI studies, photosensitizers are added to a microbial suspension from a homogeneous solution. In this methodology, after PDI treatment the photosensitizer remains in the place of action, producing an undesired photodynamic effect and contaminating the medium. In addition, under these conditions the photodynamic agent is difficult to recover for its reuse in subsequent applications. This drawback can be avoided by using photosensitizers chemically bound to a support.[7] Thus,

photosensitizers immobilized on a surface have been proposed for the inactivation of microorganisms, considering economic and ecological subjects.[8] In hospital environments, surfaces are one of the main components of possible reservoirs of bacteria, which cause a notable incidence in nosocomial infections.[1] In this way, the coating of surfaces with photosensitizers, which are immobilized in a film and can be activated by visible light, are of great interest to maintain aseptic surfaces in the public health.[9]

Porphyrin-based photosensitizers have been used to eradicated pathogenic microorganisms by irradiation with visible light.**Error! Bookmark not defined.**,[10] These compounds have demonstrated to be effective to photokilling *E. coli* and *S. aureus* in cell suspensions.[11,12] In particular, tetrapyrrolic macrocycles bearing directly attached electroactive groups, such as diphenylaminophenyl or carbazoyl substituents, are able to form polymeric films by electrodeposition.[13-15] However, interaction between porphyrins was found in the hyperbranched film structures, which negatively affects the spectroscopic and photodynamic properties of the surfaces. Therefore, in the present study a novel peripherally carbazole functionalized dendrimeric cruciform porphyrin (**DP 5**, Scheme 1) was designed and synthesized by click chemistry. The click reaction, designed to azide-alkyne 1,3-dipolar cycloaddition catalyzed by copper (CuAAC), is a well-established approach that lets to obtain complex molecular structures.[16] CuAAC is a powerfull tool to connect two molecules in an efficient and straightforward manner and have been applied in the last years in several functionalization and synthesis of dendrimers.[17-20] CuAAC reaction fulfills the requirements for porphyrin chemistry of being an available simple, efficient and versatile synthetic strategy for functionalizing porphyrin units.[21] The formation of a 1,2,3-triazole ring can be accomplished in mild reaction conditions, in a variety of solvents and affording the expected product in very good yields, besides the stereoelectronic properties of the starting materials.[22-24] Therefore, porphyrin linked by a 1,2,3-triazole unit with π-conjugated aromatic dendrons are very interesting synthetic designs and a challenging task for the development of organic materials based on the nitrogenated aromatic macrocycle. Also, constitutional components of **DP 5**, porphyrin **P 6** and carbazole **C 7**, were synthesized (Scheme 2). The electroactive carbazoyl groups in **DP 5** were used to obtain electrogenerated polymeric

film (**FDP 5**). The spectroscopic characteristics and photodynamic properties of **FDP 5** were compared with those of **DP 5** and its constitutional components, **P 6** and **C 7**. Photodynamic action sensitized by the modified surface was studied *in vitro* to eradicate *Staphylococcus aureus* and *Escherichia coli*. The development of new strategies was investigated to combat planktonic, individual and biofilm-embedded microorganisms. Thus, these studies allow determinate the efficiency of **FDP 5** as self-sterilizing agents activated by visible light.

Experimental Section

Synthesis

5,10,15,20-Tetrakis(pentafluorophenyl)porphyrin (**1**). Pentafluorobenzaldehyde (637 mg, 3.24 mmol) and pyrrole (234 μL, 3.37 mmol) were dissolved in dichloromethane (DCM) (135 mL) and purged with argon for 15 min. Then, $BF_3.OEt_2$ (50 μL, 0,40 mmol) was added and the reaction mixture was stirred a room temperature for 40 h under argon atmosphere. After addition of 2,3-dichloro-5,6-dicyano-1,4-benzoquinone (DDQ) (585 mg, 2.58 mmol), the stirring at room temperature was continued for 2 h. The solvent was evaporated under reduced pressure. The black crude product was purified by chromatography (cyclohexane/DCM, 1:1) to give porphyrin **1** (593 mg, 0.61 mmol, 19%). The spectroscopic data of **1** agree with those previously reported.[25]

5,10,15,20-Tetrakis(2,3,5,6-tetrafluoro-4-azidophenyl)porphyrin (**2**). Sodium azide (29 mg, 0.44 mmol) was added to a solution of porphyrin **1** (100 mg, 0.1 mmol) in DMF (3 mL). The reaction mixture was heated at 60 ºC for 1.5 h under an argon atmosphere. After that, 40 mL of DCM was added and the organic layer was washed with three aliquots of 25 ml of water and then dried over $MgSO_4$. The solvent was evaporated in vacuum to yield **2** as a purple solid (91 mg, 85 μmol, 83%). Porphyrin **2** was used without more purification in the next step. The spectroscopic data of **2** match with those previously reported.[26]

Zinc(II) 5,10,15,20-tetrakis(2,3,5,6-tetrafluoro-4-azidophenyl)porphyrin (**3**). A solution of porphyrin **2** (100 mg, 93 μmol) in 8 ml of DCM was stirred with 4 mL of a saturated solution of zinc(II) acetate ($Zn(AcO)_2$) in methanol. The reaction mixture was kept for 12 h under argon atmosphere at room temperature. Then, DCM (40 mL) was added and the organic phase was washed with water (30 mL x 3). The solvent was removed under reduced pressure affording porphyrin **3** (95 mg, 84 μmol, 90%). ^{1}HNMR ($CDCl_3$, TMS) δ [ppm] 9.03 (s, 8H, β-H). ^{19}FNMR ($CDCl_3$, TMS) δ [ppm] -137.34 (dd, J = 22.5, 10.0 Hz, 8 F, Ar-F_{ortho}), -151.86 (dd, J = 22.5, 10.0 Hz, 8 F, Ar-F_{meta}). ESI-MS [m/z] 1129.0240 $[M+H]^+$ (1128.0154 calculated for $C_{44}H_8F_{16}N_{16}Zn$).

Dendron **4** was synthesized according as previously published procedure.[27]

Dendrimeric porphyrin **DP 5**. Dendron **4** (38.0 mg, 0.054 mmol) and porphyrin **3** (15.0 mg, 0.011 mmol) were dissolved in a mixture of anhydrous tetrahydrofuran (THF, 5 mL) and anhydrous acetonitrile (1 mL) under argon atmosphere. CuI (5.0 mg, 0.5 equiv. per position) and *N,N*-diisopropylethylamine (DiPEA, 15 drops) were added and the reaction mixture was purged with argon. Then the reaction was heated to 60 °C and stirred for 16 h. Solvents were concentrated under vacuum and the crude product was purified by flash chromatography (hexane:DCM) yielding dendrimer **DP 5** as bright purple solid (41.8 mg, 0.013 mmol, 82%). ^{1}HNMR ($CDCl_3$, TMS) δ [ppm] 9.14 (d, J = 8.5 Hz, 8H), 8.39 (s, 4H), 8.16 (d, J = 7.7 Hz, 16H), 7.88 (s, 8H), 7.70-7.35 (m, 72H), 7.38-7.25 (m, 32H), 7.22 (d, J = 15.9 Hz, 4H), 7.12 (d, J = 15.9 Hz, 4H). ^{13}CNMR ($CDCl_3$, TMS) δ [ppm] 109.80, 119.92, 120.35, 121.88, 123.33, 124.65, 125.17, 125.93, 126.41, 127.07, 127.92, 128.13, 128.83, 132.59, 138.27, 140.70, 140.98, 146.36, 146.97, 149.99. MALDI-TOF-MS [m/z] 3934.2 $[M+H]^+$ (3933.1478 calculated for $C_{252}H_{148}F_{16}N_{28}Zn$).

Porphyrin **P 6**. Commercial phenylacetylene (40 μl, 0.36 mmol) and porphyrin **3** (20.6 mg, 0.018 mmol) were dissolved in a mixture of anhydrous THF (2.5 mL) and anhydrous acetonitrile (0.5 mL) under inert atmosphere. Then, the mixture was purged with Ar for 3 min at room temperature. Then, DiPEA (3 drops) and CuI (2.7 mg, 0.014 mmol) were added and the resulting mixture was purged with

Ar. Reaction was heated at 60 °C for 16 h. Solvents were concentrated under reduced pressure and crude product was purified by flash chromatography (hexane: dichloromethane: acetonitrile) affording **P 6** as red solid (16.7 mg, 0.011 mmol, 60%). ^{1}HNMR ($CDCl_3$, TMS) δ [ppm] 9.15 (s, 8H), 8.40 (s, 4H), 7.87 (d, *J* = 7.5, 8H), 7.47 (m, 12H). ^{13}CNMR ($CDCl_3$, TMS) δ [ppm] 122.13, 126.26, 129.26, 132.43, 140.00, 141.57, 143.43, 145.21, 148.56, 150.13, 151.73, 153.62. MALDI-TOF-MS [m/z] 1537.2 $[M+H]^+$ (1536.2032 calculated for $C_{76}H_{32}F_{16}N_{16}Zn$).

Dendron **D 7**. Phenylazide (20 μL, 0,20 mmole) and dendron **4** (48.5 mg, 0.07 mmole) were dissolved in a mixture of anhydrous THF (5 mL) and anhydrous acetonitrile (1 mL) and the solution was purged with Ar for 3 min. Then, DiPEA (10 drops) and CuI (6.2 mg, 0.032 mmol) were added and the resulting reaction mixture was purged again. Reaction was heated at 60 °C for 16 h. Solvents were concentrated under reduced pressure and crude product was purified by flash chromatography (hexane: dichloromethane) affording **D 7** as yellow solid (53.2 mg, 0.065 mmol, 93%). ^{1}HNMR ($CDCl_3$, TMS) δ [ppm] 8.21 (s, 1H), 8.16 (d, *J* = 7.7 Hz, 2H), 7.93 (d, *J* = 8.1 Hz, 2H), 7.85-7.78 (m, 2H), 7.68-7.40 (m, 24H), 7.31 (td, *J* = 7.4, 6.9, 1.6 Hz, 6H), 7.20 (d, *J* = 16.2 Hz, 1H), 7.11 (d, *J* = 16.2 Hz, 1H). ^{13}CNMR ($CDCl_3$, TMS) δ [ppm] 109.97, 117.64, 120.05, 120.50, 120.72, 123.47, 124.91, 125.25, 126.08, 126.30, 127.11, 127.46, 128.01, 128.28, 128.48, 128.98, 129.98, 132.67, 132.92, 137.75, 141.15, 146.57, 148.33. ESI-MS [m/z] 821.3405 $[M+H]^+$ (820.3314 calculated for $C_{58}H_{40}N_6$).

Film electrodeposition

Electrochemical studies were conducted in a three-electrode glass cell, using an indium tin oxide (ITO, 7x50x0.9 mm, Delta Technologies, Stillwater, MN) working electrode (Figure S1). In this configuration, the pseudo-reference electrode was a silver wire, while a Pt coil was used as counter electrode. Cyclic voltammetry (CV) measurements were done in DCM containing 0.1 M tetrabutylammonium hexafluorophosphate ($TBAPF_6$) as supporting electrolyte. The **FDP 5** films were

deposited over the mentioned ITO electrodes by CV, cycling the working electrode in a solution containing 0.5 mM **DP 5** in the -0.2 to 1.4 V range, for ten cycles at 100 mV/s.

Spectroscopic studies

UV-visible absorption and fluorescence emission measurements in *N*,*N*-dimethylformamide (DMF) were achieved as previously described.[11] The polymeric films formed on the ITO electrode were directly measured by placing the surface in the spectrometer cell holder. Fluorescence emission spectra were recorder by exciting the samples at λ_{exc}=550 nm. The energy of the singlet-state (E_s) was determined from the intersection of the normalized absorption and fluorescence bands. The fluorescence quantum yield (Φ_F) of each porphyrin was calculated using zinc(II) 5,10,15,20-tetrakis(4-methoxyphenyl)porphyrin (ZnTMP) as a reference (Φ_F=0.049) in DMF.[28]

Steady state photolysis

9,10-Dimethylanthracene (DMA, 35 μM) and the photosensitizer in DMF (2 mL) were irradiated with monochromatic light at 555 nm. A photosensitizer absorption of 0.1 was used at the irradiation wavelength. Similarly, **FDP 5** film was irradiated with a wavelength range between 455 and 800 nm. The kinetic of DMA photooxidation was analyzed by the decrease in the absorption band at λ_{max}=378 nm. The observed rate constants k_{obs}^{DMA} of DMA oxidation and quantum yields of $O_2(^1\Delta_g)$ production (Φ_Δ) of porphyrins were obtained as previously reported.[11] ZnTMP was used as a reference (Φ_Δ = 0.73).[28] Also, **FDP 5** film was irradiated at 410 nm in 2 mL water containing 9,10-anthracenediyl-bis(methylene)dimalonic acid (AMDA, 50 μM). The AMDA photooxidation was monitoring by decreasing the fluorescence emission in real-time at 430 nm.

Photobleaching measurements

FDP 5 film was irradiated in PBS or cell suspensions in PBS (~10^6 colony forming units per milliliter, CFU/mL) with visible white light as described below for PDI. The kinetics of photobleaching were investigated by decreasing of the porphyrin absorption at Soret band (430 nm). The observed rate constants (k_{obs}^P) of photobleaching were calculated from the semilogarithmic plot of ln A_0/A *vs*. irradiation time. The photodegradation lifetime (τ^P) was calculated from ln $2/k_{obs}^P$.

Strains and culture conditions

Escherichia coli ATCC 25922 and a methicillin-resistant *Staphylococcus aureus* ATCC 43300 (MRSA) were employed for PDI studies. Stock cultures were preserved in tryptic soy broth (TSB) supplemented with glycerol 10 % V/V at -80ºC. Strains were grown aerobically in tryptic soy agar (TSA) for 18 h at 37 ºC. Then, a single pure colony was collected and transfer to fresh TSB to achieve fresh cultures.

PDI of planktonic cells

Strains were grown to exponential phase in TSB at 37 ºC until the absorbance reached a value of 0.5 at 660 nm. Afterward, samples were diluted in phosphate-buffered saline (PBS, pH=7.0) solution to have a ~10^6 CFU/mL, following the McFarland standard. Next, the planktonic suspension (250 µL) was placed over **FDP 5** film or ITO electrode surface. Later, *S. aureus* and *E. coli* samples were irradiated with visible light for 15 and 30 min, respectively. Bacterial viability counts were assayed by plating 10 µL of 10-fold serial dilutions on TSA and incubated for 18 h at 37 ºC.

PDI of cells attached to the surface

Photokilling of *S. aureus* and *E. coli* was observed by propidium iodine (PI) emission. Bacterial suspension (200 µL) was transferred to the sample chamber constituted by a 5x5 mm^2 coverslip coated with a thin layer of ITO followed by electrodeposition of **DP 5**. Finally, 0.4 mm diameter cylinder was

glue to the surface. After 20 min, the bacterial excess was removed by rinsing the chamber with PBS. Then, 1 μM of the cell death marker PI in 200 μL PBS solution was added to the cells. After 15 min, photoinactivation assays started upon irradiation with white light 0.9 mW/cm^2 measured out of the objective. The images of cells were obtained as reported in literature.[29]

PDI of assembled biofilms

Biofilms of *S. aureus* and *E. coli* were induced over **FDP 5** film or ITO electrode surface in TSB supplemented with glucose 0.5 % P/V under continuous shaking (150 rpm) for 24 h at 37 ºC. The surface was rinsed three times with PBS to remove non-attached bacteria. The back of the surface without covering was cleaned mechanically with a sterile cotton swab embedded with alcohol 70% v/v. After that, the surfaces and the mature biofilms were irradiated with visible light for 60 min. The dark controls were wrapped with aluminum foil during this period. Finally, the surface was sonicated for 1 min to unpin viable cells in 5 mL PBS (~10^8 CFU/mL) and serial dilutions were performed in PBS, as described above.[30] Control tests and statistical analysis were performed in all biological experiments.[29]

Results and Discussion

Synthesis of porphyrin

A novel dendrimeric porphyrin **DP 5** was synthesized as shown in Scheme 1. The synthetic procedure started with the preparation of the free-base porphyrin **1**. The most efficient conditions to obtain **1** were those reported by Dommaschk *et* al..[25] Thus, condensation of pyrrole and pentafluorobenzaldehyde catalyzed by $BF_3.OEt_2$ in DCM was used to obtain porphyrinogen. The oxidation with DDQ at room temperature produced **1** in 19% yield after one-flask two consecutive steps. This porphyrin is a suitable and versatile building block for the construction of *meso*-substituted tetrapyrrolic macrocycles through the nucleophilic aromatic substitution reaction (S_NAr).[31] The second step was a regioselective S_NAr between **1** and of sodium azide in DMF,[26] which afforded **2** in 83% yield. After that, to finish the synthesis

of porphyrin core, a metalation reaction with $Zn(AcO)_2$ in DCM/MeOH was carried out, giving metal complex **3** in 90% yield. The progress of the reaction was observed by UV-visible absorbance spectroscopy, following the decrease of lower energy Q band in **2** (free-base porphyrin), in favor of the rise of the band at 550 nm. These spectroscopic features was correlated with the zinc(II) porphyrin formation.[32] The introduction of heavy metals in porphyrin core induce a strong spin-orbit coupling and favor the intersystem crossing from the S_1 to long-lived triplet state T_1.[33] The high triplet quantum yield is advantageous for the ROS generation.

Subsequently, porphyrin-based dendrimer **DP 5** was obtained by click reaction between **3** and **4**, which was prepared according to literature protocol.[27] This synthetic approach for Cu(I)-catalyzed azide-alkyne cycloadditions is a versatile procedure for applications in porphyrin chemistry.[34] According to our experience,[35] first click reaction assay to couple core **DP 5** and dendron **D 4** was a homogeneous condition, using the stable compound $Cu(PPh_3)_3Br$ as source of Cu(I) and DiPEA as base in anhydrous THF. However, the product isolated by flash chromatography and analyzed by NMR spectrometry was not the expected dendrimer. Based on previous reports for triazole porphyrin dimers,[34,36] we used CuI as Cu(I) source, DiPEA and a mixture of THF and acetonitrile. These reaction conditions were appropriated, affording the expected cruciform porphyrin-core dendrimer **DP 5** in 82% yield. These three reactions are robust, straightforward and with high yields. By the introduction of 4,4'-di(*N*-carbazolyl)triphenylamine units, the resulting structure has four arms, which end with two carbazole groups. Thus, these eight groups in the periphery of the tetrapyrrolic macrocycle are able to form electrogenerated polymer by the dimerization of carbazole units.[13,14]

Molecular structure of this dendrimer containing a porphyrin core was determined by NMR and MS spectra. In the aromatic region of ^{1}HNMR spectrum of **DP 5**, as a consequence of the symmetric substitution on the tetrapyrrolic ring, eight β-pyrrolic protons give rise to a singlet at 9.14 ppm. Furthermore, the aromatic protons of carbazole, triphenylamine and phenyl-vinylene moieties are overlapped in the region between 7.00 to 8.30 ppm of the ^{1}HNMR spectrum. In this region, a doublet at

8.16 ppm (J = 7.7 Hz) was observed, which belongs to carbazole ring and integrated for 16 protons according to the cruciform architecture of the porphyrin-core dendrimer **DP 5**. Other signals found were doublets at 7.12 ppm and 7.22 ppm corresponding to vinylic protons, which showed a coupling constant value of 15.9 Hz due to *trans* geometry of the alkene. A broad singlet signal at 8.39 ppm corresponding to a total of four protons demonstrated the completed formation of four triazole groups around the macrocycle. Furthermore, in the upfield region, the signal corresponding to inner pyrrolic H is absent, which confirmed that zinc(II) complexation was retained after the click reaction. In ^{13}CNMR, triazole CH carbon signal at 121.9 ppm, pyrrolic carbon at 132.9 ppm and characteristic carbazole CH carbons at 120.1, 120.5 and 110.2 ppm were observed. In addition, vinylic carbons belonging to *trans*-alkene bond at 127.2 and 129.0 ppm were also found. The *para* tetra-functionalization was confirmed by ^{19}FRMN, which showed two signals at -134 and -146 ppm that were assigned to *orto* and *meta* fluor atoms.

On the other hand, the two constitutional moieties of **DP 5** were synthesized (Scheme 2) via click chemistry in order to study and compare their properties. One of them is the porphyrin-triazole core **P 6** without the electropolymerizable units and the second is the dendron-triazole **D 7**. Both molecules were prepared using the same synthetic protocol applied to **DP 5**. Thus, porphyrin core **3** was submitted to a CuAAC reaction with excess of commercial phenylacetylene, affording **P 6** in 60% yield. Characterization by NMR and MS spectroscopies confirmed the expected structure. ^{1}HNMR spectrum of **P 6** showed a singlet at 9.15 ppm corresponding to eight β-pyrrolic protons and a singlet at 8.40 ppm belongs to four vinylic protons of the triazole ring. Phenyl ring are responsible for the doublet at 7.87 ppm and for the multiplete centered at 7.47 ppm, both signals integrated for 20 protons. Two characteristic signals of carbon were found in ^{13}CNMR spectrum: pyrrolic CH at 132.4 ppm and triazolic CH at 122.1 ppm. Also, ^{19}FNMR spectrum showed two signals at -134.8 and -146.4 ppm corresponding to C-F of the aromatic ring. Moreover, CuAAC reaction of dendron **4** with three equivalents of freshly synthesized phenyl azide yielded the expected dendron-triazole **D 7** (93%). Molecular structure was confirmed by NMR and MS

spectroscopies and the data collected were in agreement with the expected compound. ^{1}HNMR spectrum for **D 7** showed a singlet at 8.21 ppm corresponding to triazolic CH, a doublet at 8.16 ppm (J = 7.7 Hz) belongs to carbazole ring and two doublets at 7.20 and 7.11 ppm for the vinylic protons with a coupling constant of 16.2 Hz, in agreement with *trans* geometry of the double bond. In ^{13}CNMR spectrum was observed the triazolic CH at 117.6 ppm, characteristic carbazole CH at 110.0, 120.5 ppm and vinylic CH at 128.1 and 128.3 ppm, respectively.

Formation of antimicrobial surfaces

Electropolymerization depositions were carried out to form antimicrobial surfaces. CV scans of **DP 5** in DCM using $TBAPF_6$ as supporting electrolyte and an ITO working electrode are shown in Figure 1. The first anodic scan of the monomer **DP 5** presents three oxidation peaks at 0.90, 1.05, and 1.35 V. These peaks were assigned to the oxidation of the porphyrin macrocycle, triphenylamine and carbazoyl groups, respectively.[13,14] In the second anodic scan, oxidation-reduction currents began to increase and these continue to grow in subsequent cycles (Figure 1). These results indicate the formation of a film on the electrode surface. It is known that oxidation of carbazoyl groups generate unstable radical cation, which react forming dicarbazole units. **DP 5** has attached eight *N*-substituted carbazoyl groups, which possess two positions available for dimerization. Subsequent electrochemical cycling of molecules bearing carbazoyl groups produce polymers over the conductive substrates.[14,27] Therefore, during continuous anodic cycling of **DP 5** monomer a polymeric film **FDP 5** is deposited over the ITO electrode. This polymer is formed by porphyrin centers that are connected one to the other by dicarbazole units, leading to the formation of a complex three-dimensional network in which the tetrapyrrolic macrocycles are embedded.[13] An idealized polymer structure is shown in Figure S2. The formation of the **FDP 5** film on an ITO electrode are shown in Figure 2A. The optical microscope image shows the homogeneous distribution of the film (Figure 2C). In addition, the morphological characterization of the **FDP 5** film was performed by SEM. As can be observed in Figure 2E, the entire surface of ITO is covered with **FDP 5**

film, without pinholes and with some polymeric dendrites that leave the surface. The dark background shows the **FDP 5** film that cover the ITO surface, while the gray structures represent the **FDP 5** polymer formed above the film layer with a dendron-shaped structure. Thus, the electropolymerization process leads to the formation of a stable film irreversibly adhered to the surface. A further advantage to this strategy is that polymers can act as light-harvesting units and efficiently transfer the energy to the porphyrin core, which enhance the antibacterial performance.[37-39] In addition, **FDP 5** film could be obtained using flexible plastic ITO electrodes. For large area applications of the antimicrobial surface, another lower cost base electrode material can be adopted for this propose, such as stainless steel and graphited aluminum bare electrodes.[40] Moreover, if back illumination is needed, low cost transparent carbon-based nanomaterials can be also used.[41]

Absorption and fluorescence spectroscopic properties

The UV-visible absorption spectra of **DP 5** and its constitutional models **P 6** and **D 7** in DMF are shown in Figure 3. These spectra were also compared with that for **FDP 5**. The main optical characteristics of these compounds are summarized in Table 1. The spectra of **DP 5** and **P 6** show the typical Soret around 420 nm and *Q*-bands in the 500-600 nm range, characteristic of the corresponding zinc(II) substituted porphyrins.[32] The sharp absorption of Soret bands indicated that porphyrins are dissolved as monomer in this medium. The absorption of **DP 5** below 400 nm is higher than that of **P 6** due to the incidence of dendrimeric structures, whereas in the visible region the spectrum of the **DP 5** is quite similar to porphyrin **P 6**. Therefore, **DP 5** spectrum is approximately the superposition of the absorption bands corresponding to **P 6** and **D 7**, which indicates the absence of interaction between these two units in the ground state. In addition, the absorption spectra of **DP 5** and **D 7** show two main bands in the UV region of the electromagnetic spectrum, one of them around 330 nm can be attributed to the triphenylamine and carbazole units,[27] whereas the lower energy band, centered around of 380, can be attributed to a π-π* transition of the triphenylamine-vinylene segments.[42-44] Furthermore, the polymer

surface **FDP 5** essentially retained the spectroscopic properties of the porphyrin-based chromophore despite to be an extensively aggregated system. The UV-visible absorption observations also confirm the electropolymerization of the **DP 5** on the ITO electrodes. The Soret and Q bands of **FDP 5** exhibit a small red-shifted of around 7 nm in comparison with those of **DP 5** in DMF, together with a small broadening of both bands. These results indicate only slight interaction between the porphyrin units in the film structure.[14]

Fluorescence emission properties of **DP 5** and **P 6** were analyzed in DMF (Figure 4). The spectra show two bands around 595 and 647 nm, which are typical for similar *meso*-substituted zinc(II) porphyrin derivatives.[32,33] These emission bands have been assigned to $Q_x(0\text{-}0)$ and $Q_x(0\text{-}1)$ transitions. This is characteristic of porphyrins with D_{2h} symmetry, indicating that the vibronic structure of the tetrapyrrolic macrocycle remains practically unchanged upon excitation.[45] These electronic transitions have been assigned to the decays from the first singlet excited state to the first two vibrational levels of the ground state. It can be note that Q(0-0) band is a smaller transition than Q(0-1), which is distinctive of pentafluorophenyl porphyrin derivatives.[45-47] Moreover, the energy levels values of the singlet excited state (E_s) were estimated for both photosensitizers (Table 1). E_s values are comparable to those previously reported for zinc(II) porphyrins.[33] The fluorescence quantum yields (Φ_F) of the porphyrins were determined using ZnTMP as a reference (Table 1). The values of Φ_F for **DP 5** and **P 6** agree with those previously reported for similar structures.[45] Even though these values are smaller than free-base porphyrins, they can be used for quantification of porphyrin by fluorescence emission procedures.

On the other hand, compound **D 7** exhibited fluorescence emission with a band centered at 490 nm, when it was excited at the maximum wavelength of its low energy absorption bands (380 nm) in DMF (Figure S3). However, **DP 5** showed only very weak emission from the dendrimeric moiety, indicating strong quenching of the dendrimer excited singlet state by the attached zinc(II) porphyrin core. The quenching efficiency was estimated to be $\eta_q \geq 0.96$ in DMF. Therefore, in this solvent there is a

relaxation pathway that takes place from the excited singlet state of the dendrimer units to zinc(II) porphyrin.

Fluorescence excitation spectra of **DP 5** and **P 6** were obtained at λ_{em} = 648 nm in DMF. As can be shown in Figure 5, both excitation spectra were similar to the absorption spectra, which indicated that **DP 5** and **P 6** are mainly dissolved as monomers in this organic solvent. Also, excitation spectrum of **DP 5** showed an important contribution of the bands due to the absorption of dendrimer arms, indicating that energy transfer take places from the surrounding groups units to the tetrapyrrolic macrocycle.

The fluorescence spectrum of the **FDP 5** film is shown in Figure 4. The emission spectrum is characterized by a broad emission band centered at 650 nm with a shoulder at 605 nm. Both bands are red-shifted respect to the monomer in solution, in agreement with the fact that the Q bands in the film are also red-shifted. In addition, **FDP 5** presented good emission proprieties, which is no common in electrodeposited films.[13,14] Moreover, the red fluorescence emission of **FDP 5** was observed irradiating the film with UV light or by fluorescence microscopy as shown in Figure 2B and D, respectively. These results indicate that the spectroscopic properties of the porphyrin unit remain unalterable when the porphyrin is incorporated in the film and this porphyrin can be embedded in the polymer without significant aggregation. These minor spectral changes in absorbance spectrum and the fluoresce properties of the film suggest that the π-π stacking between the porphyrin cores is impede and only takes place a weak coupling interaction. This fact can be explained as result of the repulsive interactions between the polymer chains.[48] In addition, axial ligand coordination can occurs between triazole unit and the metal center on the porphyrin. Triazole group is a stable heterocycle, where the nitrogen at the 3-position has a pair of non-covalent electrons that can coordinate as axial ligand with the zinc center of a second zinc(II) porphyrin molecule.[49] This assemble between 1,2,3-triazoles and zinc(II) porphyrins tends to form a cofacial dimer both in the solid and solution states,[49] without affect the photoexcited-state processes of the porphyrin.[50,51] To summarize, the tetrapyrrolic macrocycle in **FDP 5** film retains

the spectroscopic properties of the porphyrin-based chromophore despite to be an extensively polymeric system.

Surface photostability

The photostability of the film is one of the most important requirements for antimicrobial films in order to the reusability and practical applications. Consequently, a photobleaching investigation of the electrodeposited **FDP 5** film was conducted by irradiation with visible light, under the same conditions used for the photoinactivation of microorganisms. The photodegradation was studied in PBS and *S. aureus* cell suspension, observing the decrease in absorption of the Soret band (Figure S4). Moreover, formation of new bands was not detected in the visible region. The photobleaching processes followed a first-order kinetic, as shown in Figure 6. The values of k_{obs}^{P} are (1.14±0.05) x 10^{-3} min^{-1} and (0.40±0.02) x 10^{-3} min^{-1} in PBS and *S. aureus* cell suspension, respectively. Under these conditions, the photodegradation lifetimes of **FDP 5** film were estimated in 10.1 h and 28.9 h in PBS and cell suspension, respectively. The photosensitizing efficiency exhibited a little decrease with the fluence of light, which is an advantage since can be reuse for several treatments. This photostability can be explained considering several features of the synthetic design of **DP 5**. It is well-know that tetraphenyl porphyrin and their metal complexes can undergo a ring opening upon irradiation in aqueous solutions.[52,53] However, Silva *et* al. demonstrated that the photooxidation reactions of several 2,6-disubstituted *meso*-tetraphenyl porphyrins have the chemical stability towards $O_2(^1\Delta_g)$.[54] If positions 2 and 6 on the phenyl rings are blocked, the photooxidations do not take place. This excellent stability is consequence of steric effects, which protected the porphyrin ring. In addition, photosensitizers with higher redox oxidation potentials are more difficult to undergo the photooxidative process of photobleaching.[52,55] In particular, **DP 5** has in its structure four electronwithdrawing perfluorated groups, which increase its oxidation potential and give oxidative stability towards photodegradation of the macrocycle. In addition, the encapsulation of tetrapyrrolic macrocycle in a dendritic environment in **FDP 5** offers suitable steric hindrances to avoid

its photobleaching. Thus, polymeric structure protects the porphyrin chromophore core against ROS increasing the photostability.

Photosensitized generation of $O_2(^1\Delta_g)$

Photooxidation of DMA induced by **DP 5** and **P 6** was determined in DMF. The reaction was followed by the decay of the DMA band at 379 nm due to the formation of 9,10-endoperoxide product.[28] Figure S5 shows representative results using **DP 5** as photosensitizer. The absorption bands of DMA decreased gradually under illumination in the presence of **DP 5**, **P 6** and ZnTMP; which means that $O_2(^1\Delta_g)$ was generated by all molecules. In addition, the porphyrin spectrum remains unchanged, while the absorbance of the DMA decreases with the irradiation time indicating that the macrocycle was photostable during these experiments. Since DMA quenches $O_2(^1\Delta_g)$ by chemical reaction, it was used as an approach to determinate the ability of the photosensitizers to produce $O_2(^1\Delta_g)$.[56] The values of k_{obs}^{DMA} were calculated from first-order kinetic plots of the DMA absorption with time (Figure 7). Also, the results were compared with those using ZnTMP as a reference. Table 1 summarized the values of k_{obs}^{DMA} calculated from the first order kinetic plots. As shown in Figure 7, the $O_2(^1\Delta_g)$ production was achieved at different rates depending on the porphyrins. **DP 5** is two times smaller compared to ZnTMP photosensitizer. Meanwhile, **P 6** exhibits a value of k_{obs}^{DMA} between **DP 5** and the reference. In addition, the values of Φ_Δ were determined comparing the kinetic data with that of the reference (Table 1). The Φ_Δ value obtained for **P 6** was the expected for a zinc(II) porphyrin derivative.[28,32] The dendrimeric structures in the periphery of the macrocycle in **DP 5** reduced the production of $O_2(^1\Delta_g)$. However, **DP 5** could act as light-activated antimicrobial when this porphyrin is deposited on a surface forming polymeric films.

To determine the $O_2(^1\Delta_g)$ generation sensitized by **FDP 5** film, the surface was transferred to a quartz cuvette with a solution of DMA in DMF. The decrease of the absorption band of DMA was

monitored after illumination with a wavelength range between 455 and 800 nm (Figure S6). This experiment confirms the photosensitization efficiency of these surfaces to produce $O_2(^1\Delta_g)$ under light illumination. ITO electrode without polymer was used in parallel as a control and no change were observed in absorption spectra. Also, photodecomposition of DMA sensitized by **FDP 5** was compared with that produced by ZnTMP, as a reference. As shown in Figure 8, the photodecomposition of DMA showed first-order kinetics with respect to substrate concentrations. The values of k_{obs}^{DMA} are summarized in Table 1. Photooxidation induced by **FDP 5** can be considered appropriate since $O_2(^1\Delta_g)$ generation occurs in the interface between the polymer surface and the solution. These results confirm that not only **DP 5** but also **FDP 5** film were able to produce $O_2(^1\Delta_g)$. Therefore, a contribution of a type II pathway takes place when the **FDP 5** film was exposed to visible light.

In addition, a second experience was carried out in order to demonstrate the capacity of this thin polymeric film to generate $O_2(^1\Delta_g)$ in water, using AMDA as molecular probe. Although, the lifetime of $O_2(^1\Delta_g)$ in water is about 4 μs, it was established that AMDA is an efficient acceptor of $O_2(^1\Delta_g)$ because to its high water-solubility.[57] Thus, decomposition of AMDA induced by **FDP 5** film was studied under aerobic conditions. Decrease in fluorescence emission was observed after irradiation, indicating the photodecomposition of AMDA (Figure S7). Therefore, **FDP 5** film was also able to generate $O_2(^1\Delta_g)$ in water. Thus, the photodynamic studies presented make evident that the **DP 5** moieties retained their photochemical properties after the polymerization and deposition process on ITO surface. Taking into account that the illumination with visible light of these surfaces revealed the suitability for the effective production of $O_2(^1\Delta_g)$, this **FDP 5** film was evaluated as antimicrobial surface to inactivate bacteria under different cell culture conditions.

PDI of bacteria

The photodynamic activity sensitized by **FDP 5** film was investigated *in vitro* to inactivate *S. aureus* and *E. coli* cells. These bacteria were chosen as representative of Gram-positive and Gram-negative strains of great interest due to their ability to produce nosocomial infections.[1,2] Thus, it is required to find different alternatives to prevent and eradicate infections caused by these bacteria.

First, photokilling of bacteria was studied by depositing a drop containing the cells on the polymeric **FDP 5** film. This approach based in antibiotic drop-tests can be used to evaluate the capacity of the film to inactivate bacteria that contaminate different surfaces in hospitals. In this approach, 250 μL of cell suspension (~10^6 CFU/mL) was located on polymeric film and the plate was irradiated with visible light. Figure 9 shows the survival of *S. aureus* and *E. coli* after 15 and 30 min irradiation, respectively. Control experiments indicated that the viability of bacteria was unaffected by kept the cells on the ITO (Figure 9, lines 1 and 5) or **FDP 5** film (Figure 9, lines 2 and 6) surfaces in the dark. After 15 min irradiation on ITO surface (Figure 9, lines 3), 1 log decrease was found for *S. aureus*, while a slight inactivation (<0.5 log) was detected in *E. coli* irradiated for 30 min (Figure 9, lines 7). Therefore, the increase in the killing of bacteria observed after irradiation was produced by the photosensitization effect of the polymeric **FDP 5** film. In *S. aureus*, no colony formation was detected using polymeric **FDP 5** film after 15 min irradiation (Figure 9, lines 4). This photoinactivation represents a reduction >99.9998% cell viability. This result indicates that the combination of polymeric **FDP 5** film and visible light were appropriated to photoinactivate *S. aureus*. A lower photoinactivation activity was observed in *E. coli* on polymeric **FDP 5** film, which produced 2.2 log decrease (in cell survival after 30 min irradiation (Figure 9, lines 8). This value represents a photoinactivation greater than 99.4% cell death. *E. coli* cells were more difficult to inactivate than *S. aureus* due to the nature of the envelope of Gram-negative bacteria.[6] A permeability barrier between the cell and the surrounding medium is produced by the outer membrane of Gram-negative bacteria, which restricts the penetration of ROS. On the ITO electrode without the **FDP 5** film, some inactivation occurs due to the photodynamic action of the semiconductor surface and in fact *S. aureus* was the most affected bacterium. In the presence of the **FDP 5** film, there was a complete

eradication of this Gram-positive bacterium, while this was not the case for *E. coli*. Therefore, when compared to a control without photodynamic activity, *S. aureus* was more susceptible than *E. coli* to the presence of ROS.Comparison between other surfaces containing immobilized photosensitizers is difficult mainly due to different experimental conditions. In a similar approach, it was previously determined the photoinactivation of bacteria sensitized by an electrogenerated porphyrin-fullerene C_{60} polymeric film. Even though the experiments were performed with a lower number of cells, it was necessary 30 min irradiation to produce a complete eradication of *S. aureus*.[58] Also, unlike **FDP 5** film, the porphyrin-fullerene C_{60} was not effective to photoinactivate *E. coli*, which points the **FDP 5** film as an improved surface to inactivate microbes.

Furthermore, photoinactivation of bacteria was evaluated in bacterial cells attached to the surface that contains the **FDP 5** film. Thus, cell death induced by **FDP 5** film was investigated in *S. aureus* and *E. coli* stained with PI. This compound passes through disordered areas of the dead cell membrane and binds to DNA, where it begins to emit red fluorescence.[59] In these experiments, bacterial inactivation was monitored in real-time by images of the fluorescence microscope. This approach represents an incipient contamination of bacteria on a surface. As can be seen in Figure 10, the **FDP 5** film induced a rapid cellular inactivation, which was detected by the appearance of dead cells as shown by the red emission of PI. Complete eradication of *S. aureus* and *E. coli* cells was found after 7.5 and 30 min irradiation, respectively. Thus, under these conditions the **FDP 5** film was an effective photosensitizer to inactivate *S. aureus* and *E. coli*, even using white light of low fluence rate (0.9 mW/cm^2). Therefore, the photoinactivation induced by **FDP 5** film remained elevated to killing bacteria attached to surfaces.

On the other hand, the inactivation capacity photosensitized by **FDP 5** film was evaluated against *S. aureus* and *E. coli* biofilms. Clinically important microorganisms that grow in medical devices are prone to form biofilms. These structures give them greater resistance and tolerance to antibiotics compared to their planktonic forms.[60] Therefore, biofilms represent a major health problem that contribute greatly to recalcitrant hospital infections. In this procedure, the **FDP 5** film was immersed in

a cell suspension (10^6 CFU/mL) in PBS for 18 h to produce the biofilm formation on the surface (1.0x0.7=0.7 cm^2). The biofilm on the opposite side of the polymeric **FDP 5** film was removed and the surface was irradiated with visible light for 60 min. The survival of bacteria is shown in Figure 11. No toxicity was observed in biofilms grown on ITO or **FDP 5** film kept in the dark (Figure 11, lines 1, 2 and 5, 6). After 60 min irradiation, the biofilms on ITO showed 1 log decrease of *S. aureus* survival, while it was about 0.5 log reduction of *E. coli* viability. As can be observed in Figure 11, the microorganisms were photoinactivated when the biofilms on the polymeric film **FDP 5** were exposed to visible light. Polymeric film exhibited a photosensitizing activity causing a 4.8 log decrease of *S. aureus* survival (Figure 11, lines 4). Similar result was obtained with *E. coli* biofilms (Figure 11, lines 8), which was reduced in 4.5 log. These decreases in bacterial survival represent more than 99.99% of cell photoinactivation. In contrast, a bactericidal effect was not obtained using the ITO electrode without the **FDP 5** film and the survival cells can grow rapidly regenerating a high microbial load. Therefore, these experiments show that the light in combination with polymeric film **FDP 5** was the main source of bacterial photokilling that was essential to produce a high antimicrobial action.

In all experiments, polymeric **FDP 5** film was stable and it was not detached from the ITO surface under biological experimental conditions. Also, it was reused at least three times keeping comparable photoinactivation capacities (Figure S8). After each treatment, the absorption spectroscopic analysis of the cell suspensions did not show the Soret band, characteristic of the porphyrin, indicating that the cultures were not contaminated with **DP 5** that was used to form the film. Therefore, the surfaces bearing polymeric **FDP 5** film could be used to obtain effective antibacterial surfaces that are activated by visible light.

Conclusions

The hospital environment may be contaminated with potential pathogens, which represent a high risk of disease transmission for patients. Mainly, *S. aureus* can develop resistance to antibiotics for

clinical use and survive for long periods in different media and on surfaces. Moreover, *E. coli* can cause severe and often deadly infections. In addition to the contaminated places, it can be transmitted to patients through health professionals. Therefore, new strategies are required to maintain aseptic conditions, mainly in areas of high risk of nosocomial infections. In this way, a novel triazole-porphyrin **DP 5** connected to a 4,4'-di(*N*-carbazolyl) triphenylamine group by means of a phenylenevinylene bridge was synthesized. In this structure, dendrimeric groups act as light-harvesting antennas, which allow improving the absorption of blue light and as electroactive moieties. The electrochemical oxidation of the terminal carbazolyl groups produced electrogenerated photoactive polymeric films. The procedure combines a relatively straightforward synthetic sequence of **DP 5** with good yields and a simple electrodeposition method that allowed obtaining **FDP 5** film. Also, dendrimeric units in **DP 5** can act as a visible light-harvesting antenna and singlet energy donor to zinc(II) porphyrin core enhances ROS production. The spectral features of **DP 5** were essentially preserved in **FDP 5** surface. In addition, it was demonstrated that the photodynamic properties of **DP 5** were retained in **FDP 5**. This procedure represents a versatile method to development photosensitized antimicrobial surfaces. **FDP 5** film showed high antibacterial activity to photoinactivate *S. aureus* and *E. coli* cells in different conditions, such as planktonic culture, attached cells to a surface and biofilms of bacteria. This antimicrobial polymer activated by visible light can allow controlling the microbial proliferation, preserving sterile environments on surfaces. Another advantage of **FDP 5** was that avoid the loss of photosensitizer by leaching. Therefore, **FDP 5** film can be recovered and reused from the irradiated medium, producing negligible environmental pollution. Therefore, coatings with highly stable polymeric **FDP 5** film present potential applications in healthcare environments for preventing and treating nosocomial infections.

Associated content

Supporting Information

Additional data including experimental procedures, idealized polymer chemical structure, fluorescence emission spectra, absorption spectra changes for the photobleaching, absorption spectra changes for the photooxidation of substrates, NMR and MS spectra for compounds **5-7**.

Author information

Corresponding Authors

*E-mail: edurantini@exa.unrc.edu.ar

ORCID

Daniel A. Heredia https://orcid.org/0000-0002-0667-3906

Sol R. Martínez https://orcid.org/0000-0002-0612-3605

Andrés M. Durantini https://orcid.org/0000-0002-7898-4033

M. Eugenia Pérez https://orcid.org/0000-0003-2067-8954

María I. Mangione https://orcid.org/0000-0003-4264-4392

Javier E. Durantini https://orcid.org/0000-0002-4583-8339

Miguel A. Gervaldo https://orcid.org/0000-0001-9287-5872

Luis A. Otero https://orcid.org/0000-0002-7347-8107

Edgardo N. Durantini https://orcid.org/0000-0001-8901-7543

Author Contributions

All authors discussed the results and contributed to the final manuscript. ⊥ These authors performed the design and implementation of the measurements.

Notes

The authors declare no competing financial interest.

Acknowledgements

Authors are grateful to Consejo Nacional de Investigaciones Científicas y Técnicas (CONICET, PIP-2015 1122015 0100197 CO) of Argentina, SECYT Universidad Nacional de Río Cuarto (PPI-2016 18/C460) and Agencia Nacional de Promoción Científica y Tecnológica (FONCYT, PICT-2012 0714) of Argentina for financial support. D.A.H, A.M.D., J.E.D. M.I.M., M.A.G., L.A.O. and E.N.D. are Scientific Member of CONICET. S.R.M. and M.E.P. thank to CONICET for the research fellowships.

References

(1) Jenkins, D. R. Nosocomial Infections and Infection Control. *Medicine* **2017**, *46*, 629-633.

(2) Li, Y.; Gong, Z.; Lu, Y.; Hu, G.; Cai, R.; Chen Z. Impact of Nosocomial Infections Surveillance on Nosocomial Infection Rates: A Systematic Review. *Int. J. Surg.* **2017**, *42*, 164-169.

(3) Olofsson, M.; Matussek, A.; Ehricht, R.; Lindgren, P-E.; Östgren, C. J. Differences in Molecular Epidemiology of *Staphylococcus aureus* and *Escherichia coli* in Nursing Home Residents and People in Unassisted Living Situations. *J. Hosp. Infect.* **2019**, *101*, 76-83.

(4) Frieri, M.; Kumar, K.; Boutin, A. Antibiotic Resistance. *J. Infect. Public Health* **2017**, *10*, 369-378.

(5) Rios, A. C.; Moutinho, C. G.; Pinto, F. C.; Del Fiol, F. S.; Jozala, A.; Chaud, M. V.; Vila, M. M. D. C.; Teixeira, J. A.; Balcão, V. M. Alternatives to Overcoming Bacterial Resistances: State-of-the-Art. *Microbiol. Res.* **2016**, *191*, 51-80.

(6) Durantini, A. M.; Heredia, D. A.; Durantini, J. E.; Durantini, E. N. BODIPYs to the Rescue: Potential Applications in Photodynamic Inactivation. *Eur. J. Med. Chem.* **2018**, *144*, 651-661.

(7) Spagnul, C.; Turner, L. C.; Boyle, R. W. Immobilized Photosensitizers for Antimicrobial Applications. *J. Photochem. Photobiol. B: Biol.* **2015**, *150*, 11-30.

(8) Noimark, S.; Dunnill, C. W.; Parkin, I. P. Shining Light on Materials-A Self-Sterilising Revolution. *Adv. Drug Deliver. Rev.* **2013**, *65*, 570-580.

(9) Mesquita, M. Q.; Dias, C. J.; Neves, M. G. P. M. S.; Almeida, A.; Faustino, M. A. F. Revisiting Current Photoactive Materials for Antimicrobial Photodynamic Therapy. *Molecules* **2018**, *23*, 2424-2460.

(10) Alves, E.; Faustino, M. A. F.; Neves, M. G. P. M. S.; Cunha, Â.; Nadais, H.; Almeida, A. Potential Applications of Porphyrins in Photodynamic Inactivation Beyond the Medical Scope. *J. Photochem. Photobiol. C: Photochem. Rev.* **2015**, *22*, 34-57.

(11) Ferreyra, D. D.; Reynoso, E.; Cordero, P.; Spesia, M. B.; Alvarez, M. G.; Milanesio, M. E.; Durantini, E. N. Synthesis and Properties of 5,10,15,20-Tetrakis[4-(3-*N*,*N*-dimethylaminopropoxy)phenyl]chlorin as Potential Broad-Spectrum Antimicrobial Photosensitizers. J. Photochem. Photobiol. B: Biol. **2016**, *158*, 243-251.

(12) Scanone, A. C.; Gsponer, N. S.; Alvarez, M. G.; Durantini E. N. Porphyrins Containing Basic Aliphatic Amino Groups as Potential Broad-Spectrum Antimicrobial Agents. *Photodiag. Photodyn. Ther.* **2018**, *24*, 220-227.

(13) Durantini, J.; Otero, L.; Funes, M.; Durantini, E. N.; Fungo, F.; Gervaldo, M. Electrochemical Oxidation-Induced Polymerization of 5,10,15,20-Tetrakis[3-(*N*-ethylcarbazoyl)]porphyrin. Formation and Characterization of a Novel Electroactive Porphyrin Thin Film. *Electrochim. Acta* **2011**, *56*, 4126-4134.

(14) Durantini, J.; G. M. Morales, G. M.; Santo, M.; Funes, M.; Durantini, E. N.; Fungo, F.; Dittrich, T.; Otero, L.; Gervaldo, M. Synthesis and Characterization of Porphyrin Electrochromic and Photovoltaic Electropolymers. *Org. Electron.* **2012**, *13*, 604-614.

(15) Suarez, M. B.; Durantini, J.; Santo, M.; Otero, L.; Milanesio, M. E.; Durantini, E.; Gervaldo, M. Electrochemical Generation of Porphyrin-Porphyrin and Porphyrin-C_{60} Polymeric Photoactive Organic Heterojunctions. *Electrochim. Acta* **2014**, *133*, 399-406.

(16) Tăbăcaru, A.; Furdui, B.; Ghinea, I. O.; Cârâc, G.; Dinică, R. M. Recent Advances in Click Chemistry Reactions Mediated by Transition Metal Based Systems. *Inorg. Chim. Acta* **2017**, *455*, 329-349.

(17] Xi, W.; Scott, T. F.; Kloxin, C. J.; Bowman, C. N. Click Chemistry in Materials Science. *Adv. Funct. Mater.* **2014**, *24*, 2572-2590.

(18) Arseneault, M.; Wafer, C.; Morin, J.-F. Recent Advances in Click Chemistry Applied to Dendrimer Synthesis. *Molecules* **2015**, *20*, 9263-9294.

(19) Marrocchi, A.; Facchetti, A.; Lanari, D.; Santoro, S.; Vaccaro, L. Click-Chemistry Approaches to π-Conjugated Polymers for Organic Electronics Applications. *Chem. Sci.* **2016**, *7*, 6298-6308.

(20) Sowinska, M.; Urbanczyk-Lipkowska, Z. Advances in the Chemistry of Dendrimers. *New J. Chem.* **2014**, *38*, 2168-2203.

(21) Ladomenou, K.; Nikolaou, V.; Charalambidis, G.; Coutsolelos, A. G. "Click"-Reaction: an Alternative Tool for New Architectures of Porphyrin Based Derivatives. *Coord. Chem. Rev.* **2016**, *306*, 1-42.

(22) Kolb, H. C.; Finn, M. G.; Sharpless, K. B. Click Chemistry: Diverse Chemical Function from a Few Good Reactions. *Angew. Chem. Int. Ed.* **2001**, *40*, 2004-2021.

(23) Bock, V. D.; Hiemstra, H.; van Maarseveen, J. H. Cu^{I}-Catalyzed Alkyne-Azide "Click" Cycloadditions from a Mechanistic and Synthetic Perspective. *Eur. J. Org. Chem.* **2006**, *1*, 51-68.

(24) Shen, D. M.; Liu, C.; Chen, Q. Y. Synthesis and Versatile Reactions of β-Azidotetraarylporphyrins. *Eur. J. Org. Chem.* **2007**, *9*, 1419-1422.

(25) Dommaschk, M.; Gutzeit, F.; Boretius, S.; Haag, R.; Herges, R. Coordination-Induced Spin-State-Switch (CISSS) in Water. *Chem. Commun.* **2014**, *50*, 12476-12478.

(26) Golf, H. R. A.; Reissig, H-U.; Wiehe A. Regioselective Nucleophilic Aromatic Substitution Reaction of *meso*-Pentafluorophenyl-Substituted Porphyrinoids With Alcohols. *Eur. J. Org. Chem.* **2015**, *7*, 1548-1568.

(27) Mangione, M. I.; Spanevello, R. A.; Minudri, D.; Cavallo, P.; Fungo, F. Electrochemical Films Deposition and Electro-Optical Properties of bis-Carbazol-Triphenylamine End-Caped Dendrimeric Polymers. *Electrochim. Acta* **2018**, *263*, 585-595.

(28) Milanesio, M. E.; Alvarez, M. G.; Yslas, E. I.; Borsarelli, C. D.; Silber, J. J.; Rivarola, V.; Durantini, E. N. Photodynamic Studies of Metallo 5,10,15,20-Tetrakis(4-methoxyphenyl) Porphyrin: Photochemical Characterization and Biological Consequences in A Human Carcinoma Cell Line. *Photochem. Photobiol.* **2001**, *74*, 14-21.

(29) Agazzi, M. L.; Durantini, J. E.; Gsponer, N. S.; Durantini, A. M.; Bertolotti, S. G.; Durantini E. N. Light-Harvesting Antenna and Proton-Activated Photodynamic Effect of a Novel BODIPY-Fullerene C_{60} Dyad as Potential Antimicrobial Agent. *ChemPhysChem* **2019**, *20*, 1110-1125

(30) Mamone, L.; Ferreyra, D. D.; Gándara, L.; Di Venosa, G.; Vallecorsa, P.; Sáenz, D.; Calvo, G.; Batlle, A.; Buzzola, F.; Durantini, E. N.; Casas, A. Photodynamic Inactivation of Planktonic and Biofilm Growing Bacteria Mediated by a *meso*-Substituted Porphyrin Bearing Four Basic Amino Groups. *J. Photochem. Photobiol. B: Biol.* **2016**, *161*, 222-229.

(31) Bhupathiraju, N. V. S. D. K.; Rizvi, W.; Batteas, J. D.; Drain, C. M. Fluorinated Porphyrinoids as Efficient Platforms for New Photonic Materials, Sensors, and Therapeutics. *Org. Biomol. Chem.* **2016**, *14*, 389-408.

(32) Scalise, I.; Durantini, E. N. Photodynamic Effect of Metallo 5-(4-Carboxyphenyl)-10,15,20-tris(4-methylphenyl)porphyrins in Biomimetic AOT Reverse Micelles Containing Urease, *J. Photochem. Photobiol. A: Chem.* **2004**, *162*, 105-113.

(33) Milanesio, M. E.; Alvarez, M. G.; Bertolotti, S. G.; Durantini, E. N. Photophysical Characterization and Photodynamic Activity of Metallo 5-(4-(Trimethylammonium)phenyl)-10,15,20-tris(2,4,6-trimethoxyphenyl)porphyrin in Homogeneous and Biomimetic Media. *Photochem. Photobiol. Sci.* **2008**, *7*, 963-972.

(34) Sheti, V. S.; Ravikanth, M. Synthesis of Triazole-Bridged Unsymmetrical Porphyrin Dyads and Porphyrin-Ferrocene Conjugates. *Eur. J. Org. Chem.* **2010**, *3*, 494-508.

(35) Mangione, M. I.; Spanevello, R. A.; Anzardi, M. B. Efficient and Straightforward Click Synthesis of Structurally Related Dendritic Triazoles. *RSC Advances* **2017**, *7*, 47681-47688.

(36) Punidha, S.; Sinha, J.; Kumar, A.; Ravikanth, M. First Triazole-Bridged Unsymmetrical Porphyrin Dyad Via Click Chemistry. *J. Org. Chem.* **2008**, *73*, 323-326.

(37) Chen, J.; Shan, J.; Xu, Y.; Su, P.; Tong, L.; Yuwen, L.; Weng, L.; Bao, B.; Wang, L. Polyhedral Oligomeric Silsesquioxane (POSS)-Based Cationic Conjugated Oligoelectrolyte/Porphyrin for Efficient Energy Transfer and Multiamplified Antimicrobial Activity. *ACS Appl. Mater. Interfaces* **2018**, *10*, 34455-34463.

(38) Xing, C.; Xu, Q.; Tang, H.; Liu, L.; Wang, S. Conjugated Polymer/Porphyrin Complexes for Efficient Energy Transfer and Improving Light-Activated Antibacterial Activity. *J. Am. Chem. Soc.* **2009**, *131*, 13117-13124.

(39) Liu, L.; Chen, J.; Wang, S. Flexible Antibacterial Film Deposited with Polythiophene-Porphyrin Composite. *Adv. Healthcare Mater.* **2013**, *2*, 1582-1585.

(40) Maerten, C.; Jierry, L.; Schaaf, P.; Boulmedais F. Review of Electrochemically Triggered Macromolecular Film Buildup Processes and Their Biomedical Applications. *ACS Appl. Mater. Interfaces* **2017**, *9*, 28117-28138.

(41) Lee, J.; Lim, M.; Yoon, J.; Kim, M. S.; Choi, B.; Kim, D. M.; Kim, D. H.; Park, I.; Choi S-J. Transparent, Flexible Strain Sensor Based on a Solution-Processed Carbon Nanotube Network. *ACS Appl. Mater. Interfaces* **2017**, *9*, 26279-26285.

(42) Xia, H. J.; He, J. T.; Peng, P.; Zhou, Y. H.; Li, Y. W.; Tian, W. J. Synthesis and Photophysical Properties Of Triphenylamine-Based Dendrimers with 1,3,5-Triphenylbenzene Cores. *Tetrahedron Lett.* **2007**, *48*, 5877-5881.

(43) Yang, Z.; Xu, B.; He, J.; Xue, L.; Guo, Q.; Xia, H.; Tian, W. Solution-Processable and Thermal-Stable Triphenylamine-Based Dendrimers with Truxene Cores as Hole-Transporting Materials for Organic Light-Emitting Devices. *Org. Electron.* **2009**, *10*, 954-959.

(44) Mangione, M. I.; Spanevello, R. A.; Rumbero, A.; Heredia, D. A.; Marzari, G.; Fernandez, L.; Otero, L.; Fungo, F. Electrogenerated Conductive Polymers from Triphenylamine End-Capped Dendrimers. *Macromolecules* **2013**, *46*, 4754-4763.

(45) Spellane, P. J.; Gouterman, M.; Antipas, A.; Kim, S.; Liu, Y. C. Porphyrins. 40. Electronic Spectra and Four-Orbital Energies of Free-Base, Zinc, Copper, and Palladium Tetrakis(perfluorophenyl)porphyrins. *Inorg. Chem.* **1980**, *19*, 386-391.

(46) Hewage, N.; Yang, B.; Agrios, A. G.; Brückner, C. Introduction of Carboxylic Ester and Acid Functionalities to *meso*-Tetrakis(pentafluorophenyl)porphyrin and Their Limited Electronic Effects on the Chromophore. *Dyes Pigm.* **2015**, *121*, 159-169.

(47) Heredia, D. A.; Durantini, A. M.; Sarotti, A. M.; Gsponer, N. S.; Ferreyra, D. D.; Bertolotti, S. G.; Milanesio, M. E.; Durantini, E. N. Proton-Dependent Switching of A Novel Amino Chlorin Derivative as a Fluorescent Probe and Photosensitizer for Acidic Media. *Chem. Eur. J.* **2018**, *24*, 5950-5961.

(48) Quan, W.-D.; Pitto-Barry, A.; Baker, L. A.; Stulz, E.; Napier, R.; O'Reilly, R. K.; Stavros, V. G. Retaining Individualities: the Photodynamics of Self-Ordering Porphyrin Assemblies. *Chem. Commun.* **2016**, *52*, 1938-1941.

(49) Maeda, C.; Yamaguchi, S.; Ikeda, C.; Shinokubo, H.; Osuka, A. Dimeric Assemblies from 1,2,3-Triazole-Appended Zn(II) Porphyrins with Control of NH-Tautomerism in 1,2,3-Triazole. *Org. Lett.* **2008**, *10*, 549-552.

(50) Maeda, C.; Kim, P.; Cho, S.; Park, J. K.; Lim, J. M.; Kim, D.; Vura-Weis, J.; Wasielewski, M.; Shinokubo, H.; Osuka, A. Large Porphyrin Squares from the Self-Assembly of *meso*-Triazole-Appended L-Shaped *meso-meso*-Linked Zn^{II}-Triporphyrins: Synthesis and Efficient Energy Transfer. *Chem. Eur. J.* **2010**, *16*, 5052-5061.

(51) Roberts, D. A.; Schmidt, T. W.; Crossley, M. J.; Perrier, S. Tunable Self-Assembly of Triazole-Linked Porphyrin-Polymer Conjugates. *Chem. Eur. J.* **2013**, *19*, 12759-12770.

(52) Bonnett, R.; Martínez, G.; Photobleaching of Sensitisers Used in Photodynamic Therapy. *Tetrahedron* **2001**, *57*, 9513-9547.

(53) Bonnett, R.; Martínez, G. Photobleaching of Compounds of the 5,10,15,20-Tetrakis(*m*-hydroxyphenyl)porphyrin series (*m*-THPP, *m*-THPC, and *m*-THPBC). *Org. Lett.* **2002**, *4*, 2013-2016.

(54) Silva, A. M.; Neves, M. G.; Martins, R. R.; Cavaleiro, J. A.; Boschi, T.; Tagliatesta, P. Photo-oxygenation of *meso*-Tetraphenylporphyrin Derivatives: the Influence of the Substitution Pattern and Characterization of the Reaction Products. *J. Porphyrins Phtalocyanines* **1998**, *2*, 45-51.

(55) Kuznetsova, N. A.; Kaliya, O. L. Oxidative Photobleaching of Phthalocyanines in Solution. *J. Porphyrins Phthalocyanines* **2012**, *16*, 705-712.

(56) Gomes, A.; Fernandes, E.; Lima, J. L. F. C. Fluorescence Probes Used for Detection of Reactive Oxygen Species. *J. Biochem. Biophys. Methods* **2005**, *65*, 45-80.

(57) Alvarez, M. G.; Gómez, M. L.; Mora, S. J.; Milanesio, M. E.; Durantini, E. N. Photodynamic Inactivation of *Candida albicans* Using Bridged Polysilsesquioxane Films Doped with Porphyrin. *Bioorg. Med. Chem.* **2012**, *20*, 4032-4039.

(58) Ballatore, M. B.; Durantini, J.; Gsponer, N. S.; Suarez, M. B.; Gervaldo, M.; Otero, L.; Spesia, M. B.; Milanesio, M. E.; Durantini, E. N. Photodynamic Inactivation of Bacteria Using Novel Electrogenerated Porphyrin-Fullerene C_{60} Polymeric Films. *Environ. Sci. Technol.* **2015**, *49*, 7456-7463.

(59) D'Incecco, P.; Ong, L.; Gras, S.; Pellegrino, L. A Fluorescence *in situ* Staining Method for Investigating Spores and Vegetative Cells of Clostridia by Confocal Laser Scanning Microscopy and Structured Illuminated Microscopy. *Micron* **2018**, *110*, 1-9.

(60) Kumara, A.; Alama, A.; Ranib, M.; Ehteshamc, N. Z.; Hasnain, S. E. Biofilms: Survival and Defense Strategy for Pathogens. *Int. J. Med. Microbiol.* **2017**, *307*, 481-489.

Table 1. Spectroscopic and photodynamic properties of porphyrins in DMF and **FDP 5** film.

Compound	λ_{max}^{Abs} (nm)	λ_{max}^{Em} (nm)	E_s (eV) [a]	Φ_F [b]	k_{obs}^{DMA} (s^{-1}) [c]	Φ_Δ [f]
DP 5	423/552	596/648	2.16	0.017±0.002	(2.16±0.02) x 10^{-4} [d]	0.27±0.02
P 6	422/552	594/645	2.16	0.026±0.002	(6.10±0.05) x 10^{-4} [d]	0.76±0.03
FDP 5	430/560	605/650	2.13	-	(4.24±0.04) x 10^{-4} [e]	

[a] energy levels of the singlet excited stated; [b] fluorescence quantum yield; [c] observed rate constants for DMA photooxidation; [d] λ_{irr} = 555 nm, reference ZnTMP, k_{obs}^{DMA} = (5.80±0.04) x 10^{-4} s^{-1}; [e] λ_{irr} = 455-800 nm, reference ZnTMP, k_{obs}^{DMA} = (3.25±0.03) x 10^{-3} s^{-1}; [f] $O_2(^1\Delta_g)$ quantum yield, reference ZnTMP $\Phi_\Delta = 0.73$.[28]

Figures and Schemes captions

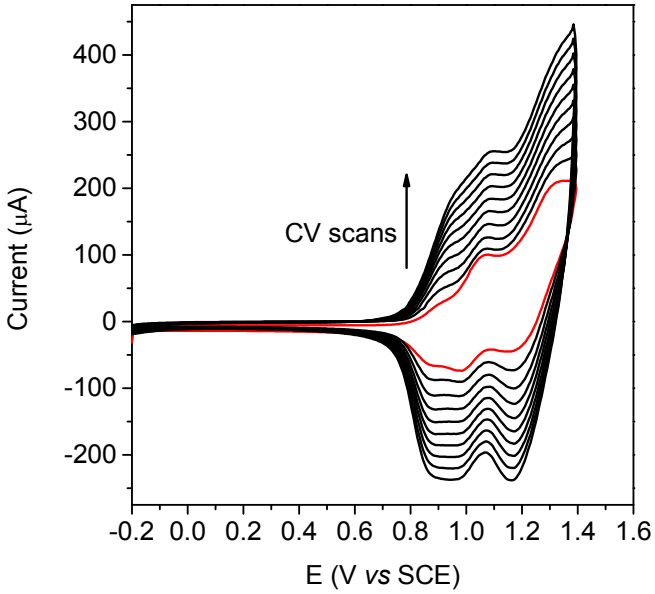

Figure 1. CV scans of **DP 5** recorded in DCM containing 0.1 M $TBAPF_6$ using an ITO working electrode. Red lines after deposition of the first layer. All the CVs were obtained at a scan rate of 100 mV/s.

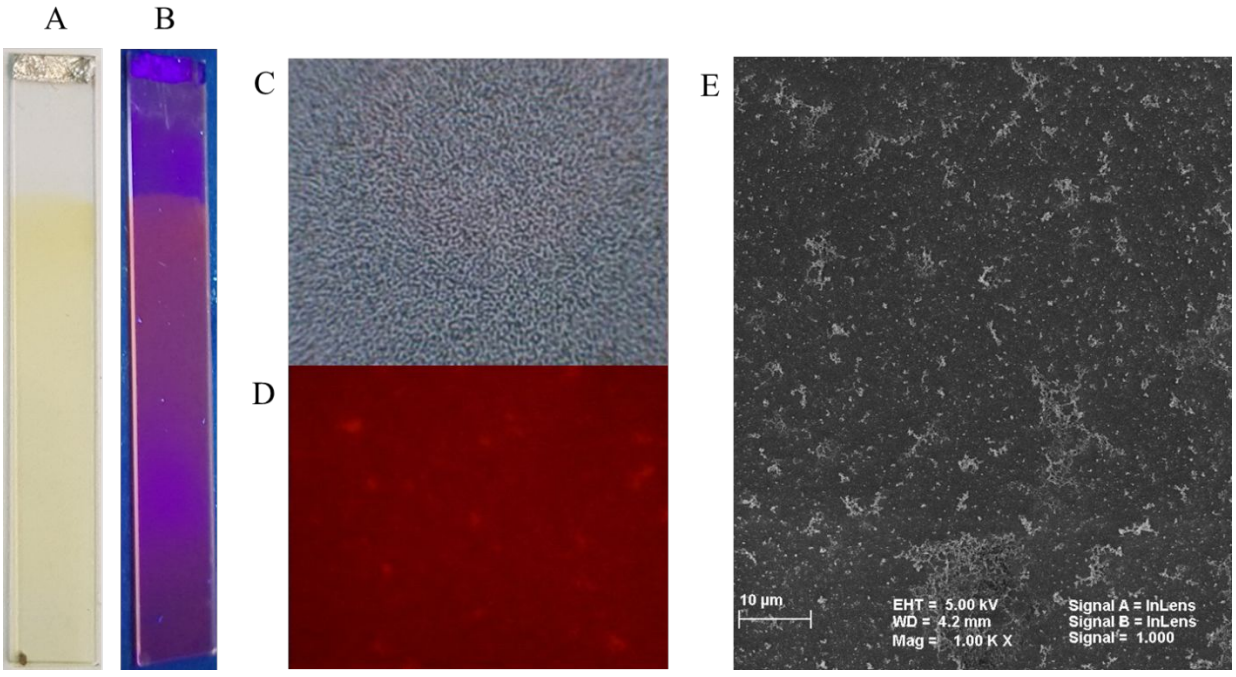

Figure 2. Photograph of the film **FDP 5** (A) irradiated with visible light and (B) exposed to UV light (λ_{exc} = 254 nm); and microscope images (40x microscope objective) (C) film under bright field and (D) fluorescence emission; (E) SEM image of **FDP 5** film (scale bar 10 µm).

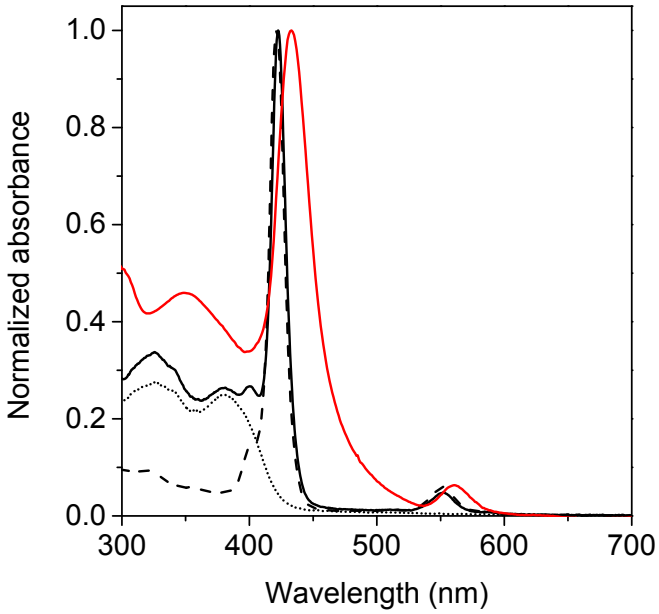

Figure 3. Absorption spectra of **DP 5** (solid line) **P 6** (dashed line) and **D 7** (dotted line) in DMF and FDP **5** film (red line).

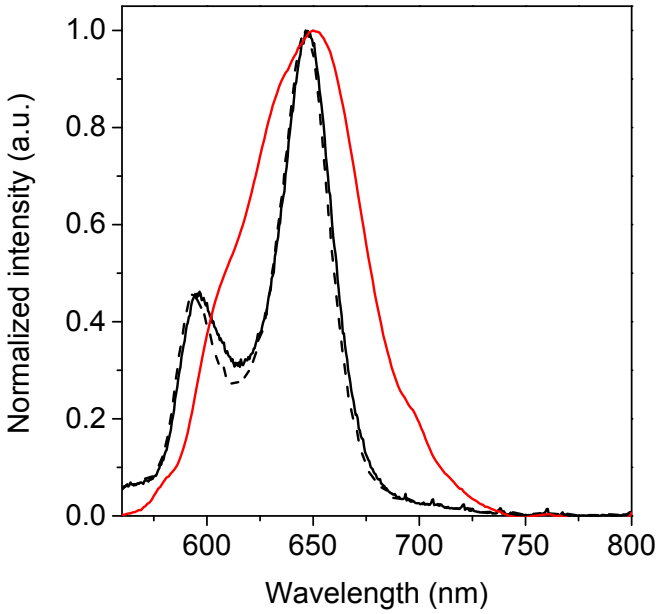

Figure 4. Fluorescence emission spectra of **DP 5** (solid line) and **P 6** (dashed line) in DMF and **FDP 5** film (red line), λ_{exc} = 550 nm.

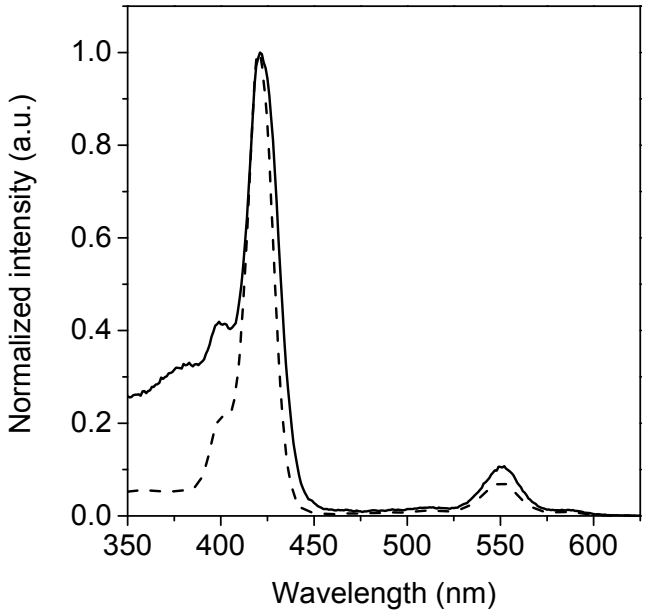

Figure 5. Fluorescence excitation spectra of **DP 5** (solid line) and **P 6** (dashed line) in DMF, λ_{em} = 648 nm.

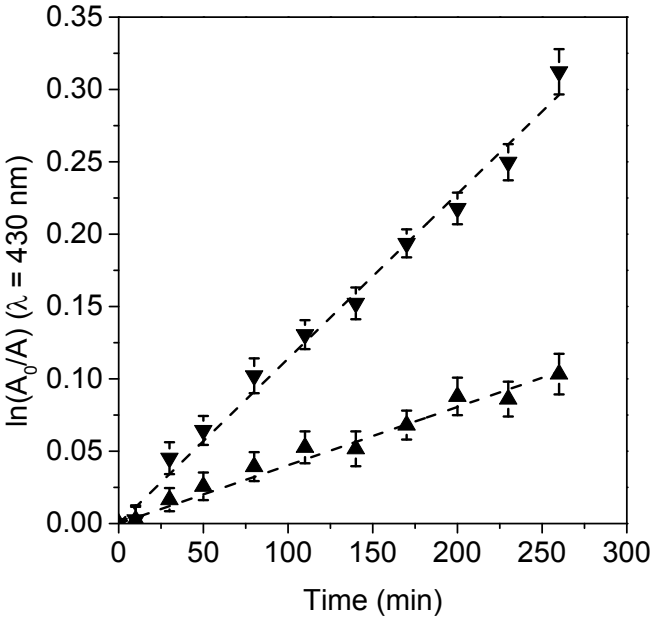

Figure 6. First-order plots for the photobleaching of **FDP 5** film irradiated with visible light in PBS (▼) and *S. aureus* cell suspension (▲).

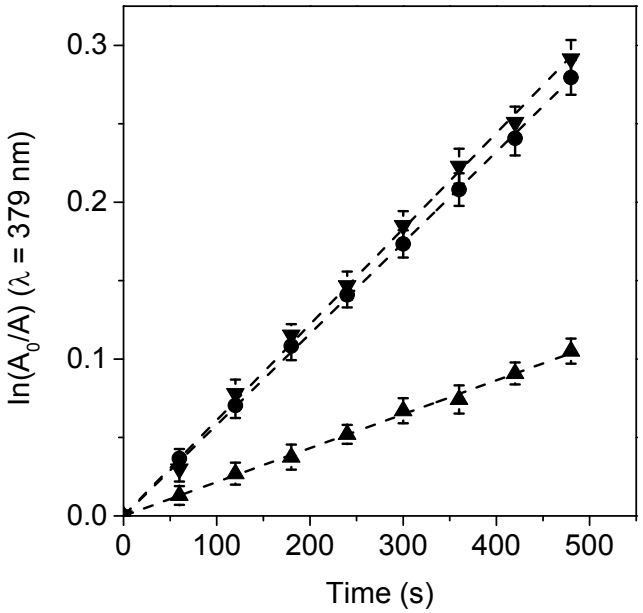

Figure 7. First-order plots for the photooxidation of DMA (20 μM) photosensitized by **DP 5** (▲), **P 6** (▼) and ZnTMP (●) in DMF, λ_{irr} = 555 nm.

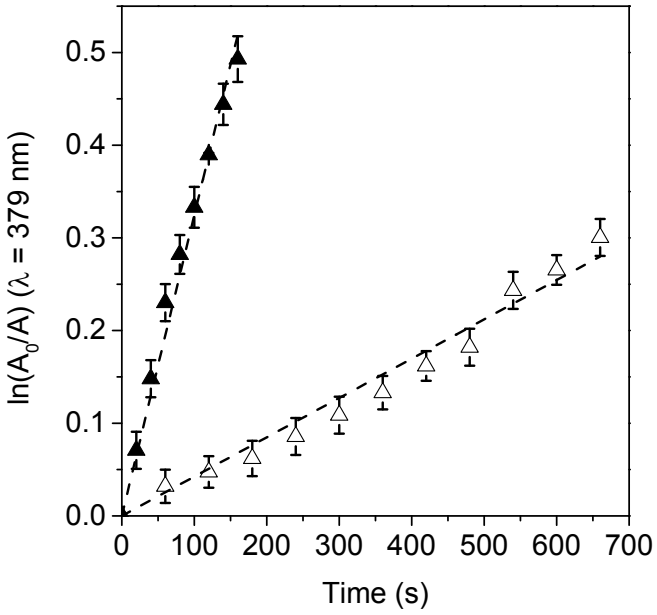

Figure 8. First-order plots for the photooxidation of DMA (20 μM) photosensitized by **DP 5** (▲) and **FDP 5** film (△) in DMF, λ_{irr} = 455-800 nm.

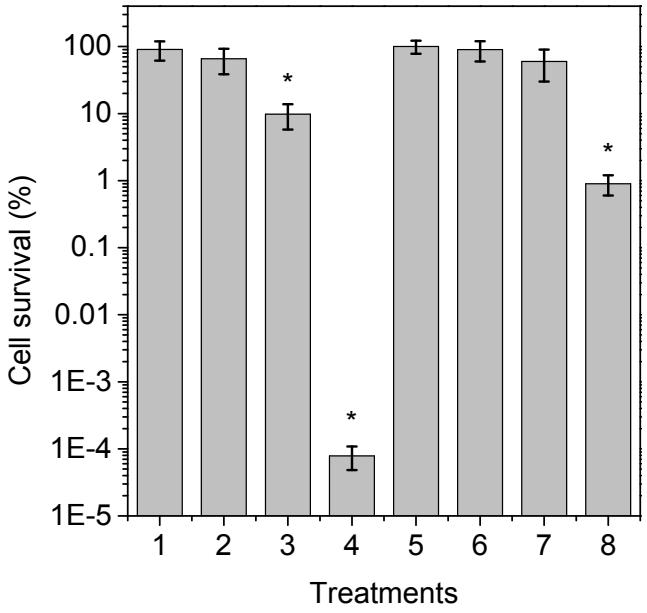

Figure 9. Survival of bacteria (~10^6 CFU/mL) depositing a drop (250 μL) with the cells on the polymeric film **5**; 1) *S. aureus* on ITO in dark; 2) *S. aureus* on **FDP 5** film in dark; 3) irradiated *S. aureus* on ITO; 4) irradiated *S. aureus* on **FDP 5** film; 5) *E. coli* on ITO in dark; 6) *E. coli* on **FDP 5** film in dark; 7) irradiated *E. coli* on ITO; 8) irradiated *E. coli* on **FDP 5** film. *S. aureus* and *E. coli* were exposed to visible light for 15 and 30 min irradiation, respectively (*$p < 0.05$, compared with control).

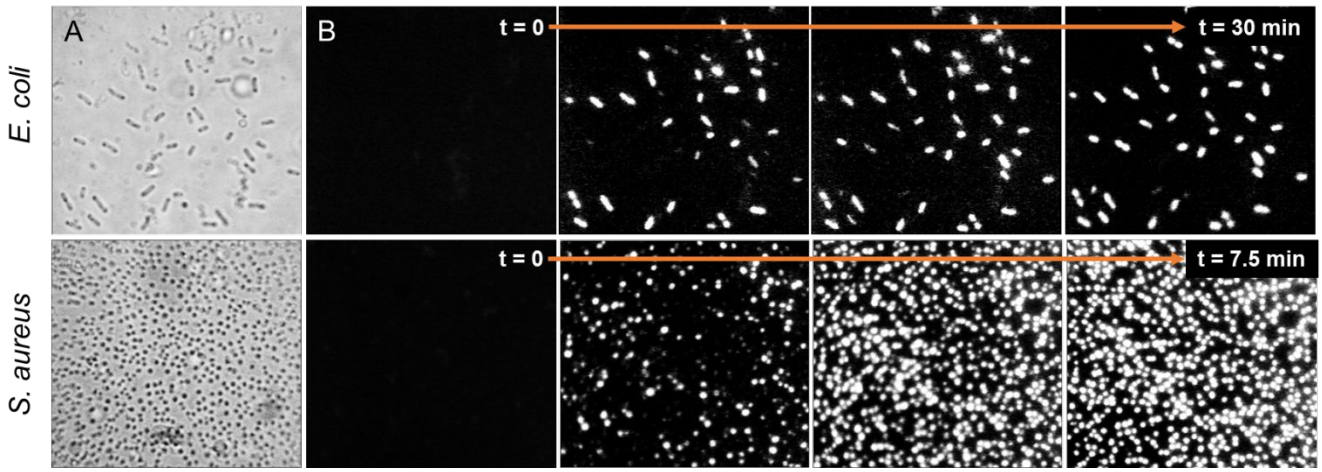

Figure 10. Microscopic images of *E. coli* and *S. aureus* incubated with 1 μM PI for 15 min in the dark on the **FDP 5** film; (A) cells under bright field at t = 0 min, (B) fluorescence emission of PI after different irradiation times. *E. coli* t = 0, 10, 20 and 30 min; *S. aureus* t = 0, 2.5, 5, 7.5 min (100×microscope objective).

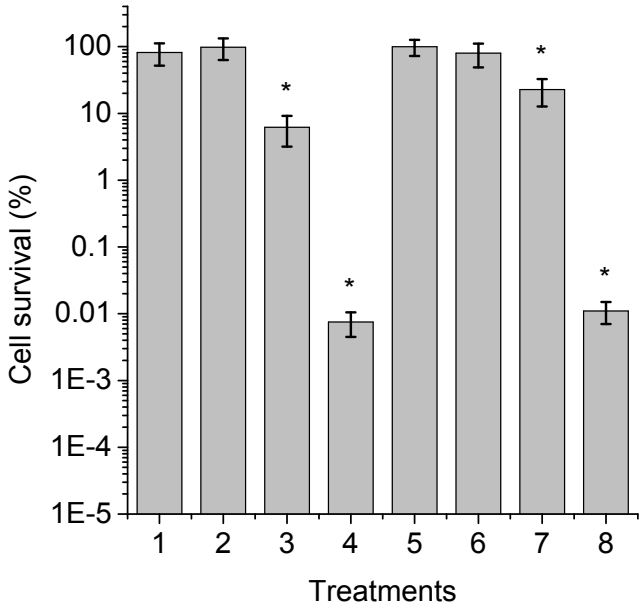

Figure 11. Survival of bacteria biofilms formed on the polymeric **FDP 5** film; 1) *S. aureus* on ITO in dark; 2) *S. aureus* on **FDP 5** film in dark; 3) irradiated *S. aureus* on ITO; 4) irradiated *S. aureus* on **FDP 5** film; 5) *E. coli* on ITO in dark; 6) *E. coli* on **FDP 5** film in dark; 7) irradiated *E. coli* on ITO; 8) irradiated *E. coli* on **FDP 5** film. *S. aureus* and *E. coli* were exposed to visible light for 60 min (*$p <$ 0.05, compared with control).

Scheme 1. Synthesis of **1-DP 5**.

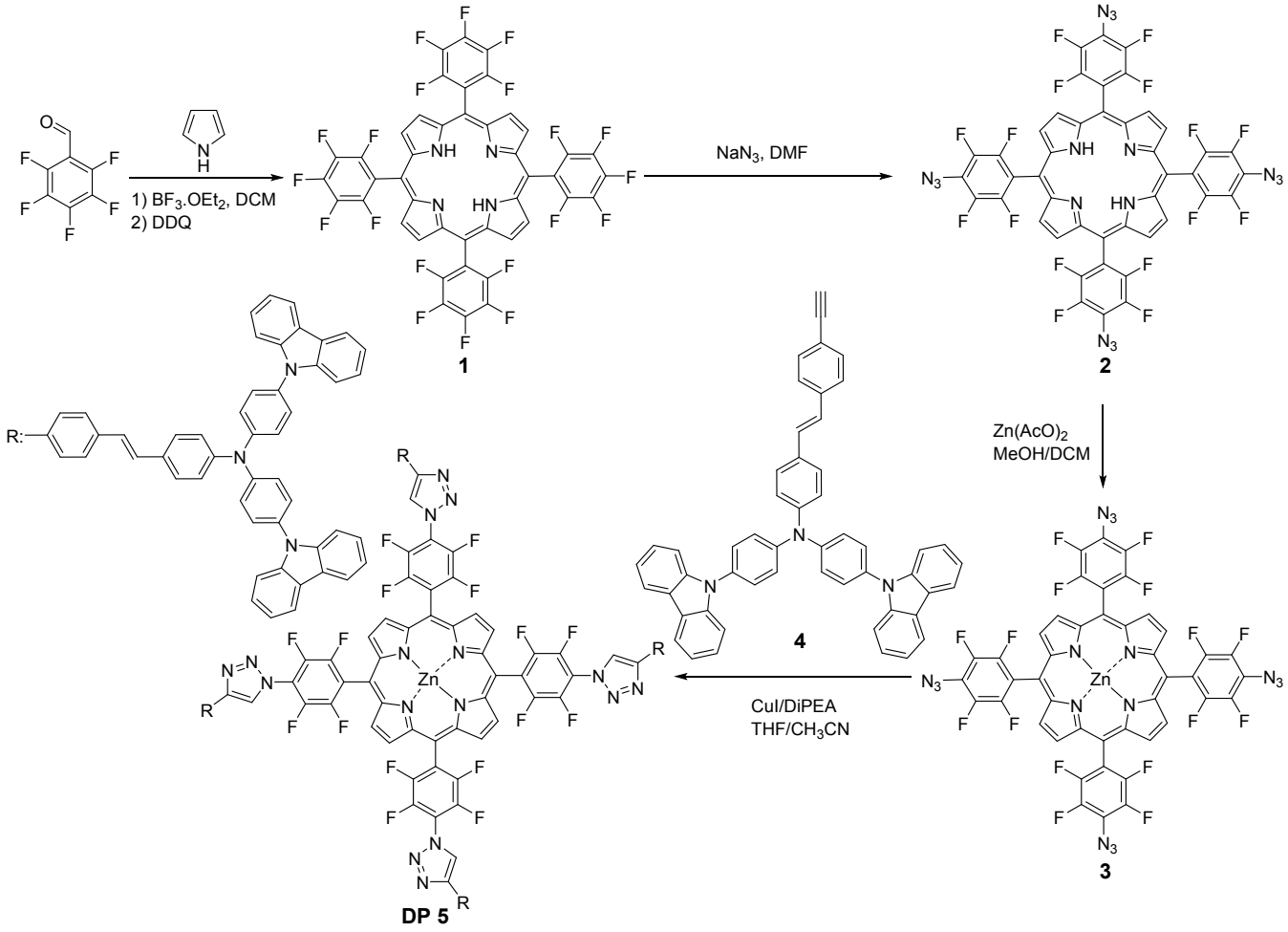

Scheme 2. Synthesis of **P 6** and **D 7**.

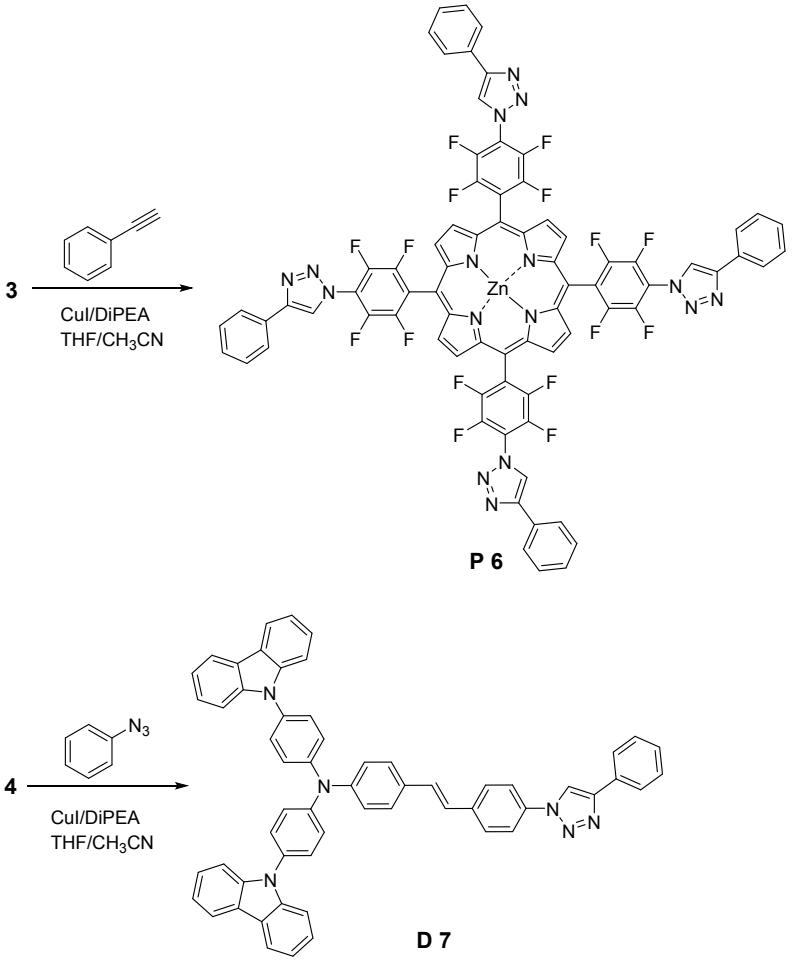

Table Of Contents (TOC)